



Share Your Innovations through JACS Directory

# Journal of Nanoscience and Technology

Visit Journal at <https://www.jacsdirectory.com/jnst>

ISSN: 2455-0191



## Silver-Modified $\text{Co}_3\text{O}_4$ Nanoparticles: Cost-Effective Synthesis, Structural Properties and Photocatalytic Degradation of EBT Dye

Rohit S. Shinde<sup>1,\*</sup>, Bhatu S. Desale<sup>1</sup>, Gokul R. Deore<sup>1</sup>, Rahul A. Shinde<sup>2</sup>, Avinash U. Nerkar<sup>3</sup>, Vishnu A. Adole<sup>4</sup>, Ravindra H. Waghchaure<sup>5</sup>, Thansing B. Pawar<sup>4</sup>

<sup>1</sup>Department of Chemistry, M.G.V's Arts, Science and Commerce College, Manmad, Nashik – 423 104, Maharashtra, India.

<sup>2</sup>Dept. of Chemistry, M.G.V's M.S.G. Arts, Science and Commerce College, Malegaon Camp, Malegaon, Nashik – 423 105, Maharashtra, India.

<sup>3</sup>Department of Chemistry, M.P.H. Arts, Science and Commerce Mahila Mahavidyalay Malegaon – 423 105, Maharashtra, India.

<sup>4</sup>Dept. of Chemistry, M.G.V's Loknete Vyankatrao Hiray Arts, Science and Commerce College, Panchavati, Nashik – 422 003, Maharashtra, India.

<sup>5</sup>Department of Chemistry, Mahant Jamanadas Maharaj, Arts, Commerce and Science College, Karanjali, Nashik – 422 003, Maharashtra, India.



### ARTICLE DETAILS

#### Article history:

Received 24 February 2026

Accepted 11 March 2026

Available online 15 April 2026

#### Keywords:

Ag/ $\text{Co}_3\text{O}_4$  NPs

Co-Precipitation

Photocatalysis

### ABSTRACT

Silver-modified cobalt oxide (5% Ag/ $\text{Co}_3\text{O}_4$ ) nanoparticles were successfully synthesized via a simple and cost-effective co-precipitation method. X-ray diffraction (XRD) confirmed the formation of crystalline spinel  $\text{Co}_3\text{O}_4$  with an average crystallite size of 18.01 nm. FE-SEM analysis revealed nearly spherical morphology, while EDS verified the successful incorporation of Ag into the  $\text{Co}_3\text{O}_4$  matrix. FT-IR spectra showed characteristic Co–O stretching vibrations at 668.39 and 568.89  $\text{cm}^{-1}$ . UV-DRS analysis indicated an optical band gap of 3.01 eV. The photocatalytic activity of the synthesized nanocomposite was evaluated through degradation of Eriochrome Black T (EBT) dye under visible light irradiation. Under optimized conditions (pH 6, catalyst dose 1 g/L), the catalyst achieved approximately 75% dye degradation. The enhanced photocatalytic performance is attributed to improved light absorption and reduced charge carrier recombination due to Ag incorporation. These findings demonstrate that 5% Ag/ $\text{Co}_3\text{O}_4$  nanoparticles are an efficient and promising photocatalyst for wastewater treatment applications.

### 1. Introduction

Organic contaminants have been widely released into aquatic systems as a result of rapid urbanization and industrialization, raising serious health and environmental issues. The textile, leather, paper, plastic, and cosmetic industries release synthetic dyes, which are especially dangerous among these pollutants because of their complex aromatic compounds, high stability, and resistance to typical biological disintegration. In addition to giving water bodies a vibrant hue, these dyes also block light, upsetting aquatic ecosystems and endangering living things by causing mutagenic, carcinogenic, and poisonous effects. In light of this, creating practical, economical, and ecologically safe methods for getting rid of these persistent pollutants has taken on significant research importance [1-5].

The capacity of semiconductor-based photocatalysis to fully mineralize organic contaminants into innocuous end products like  $\text{CO}_2$  and  $\text{H}_2\text{O}$  under light irradiation has made it a viable advanced oxidation technique for wastewater treatment. The high surface-to-volume ratio, adjustable band gap, superior chemical stability, and robust redox potential of metal oxide nanomaterials have garnered a lot of interest in this subject. They are appropriate for a variety of uses, including as gas sensing, catalysis, electrochemical energy storage, optoelectronics, and environmental remediation, due to their dynamic electronic structure, which enables to display metallic, semiconducting, or insulating characteristics [6-9].

$\text{Co}_3\text{O}_4$  is one of the transition metal oxides that has been studied the most because of its special structural, electrical, and catalytic characteristics. The p-type semiconductor  $\text{Co}_3\text{O}_4$  has a conventional spinel crystal structure, with tetrahedral and octahedral positions occupied by  $\text{Co}^{2+}$  and  $\text{Co}^{3+}$  ions respectively. Because of its mixed valence state, which speeds up electron transport and increases redox activity,  $\text{Co}_3\text{O}_4$  is a useful material for gas sensors, lithium-ion batteries, supercapacitors, electrochromic devices, and heterogeneous catalysis. Furthermore,  $\text{Co}_3\text{O}_4$  has a large theoretical capacity, low cost, good chemical stability, and

environmental compatibility. Because of these characteristics, it could be used in photocatalytic applications [10-13].

However, some intrinsic disadvantages, such as the quick recombination of photogenerated electron-hole pairs, the comparatively small surface area, and the limited absorption of light in the visible spectrum, limit the practical photocatalytic efficacy of pure  $\text{Co}_3\text{O}_4$ . Numerous modification techniques, including morphological control, composite synthesis, and metal ion doping, have been investigated in an effort to get beyond these restrictions and improve its photocatalytic efficacy. Noble metal alteration has shown to be the most successful of these strategies. Because silver (Ag) nanoparticles (NPs) create a Schottky barrier at the metal-semiconductor interface, their incorporation into the  $\text{Co}_3\text{O}_4$  matrix can greatly increase the efficiency of charge separation. Additionally, Ag NPs have surface plasmon resonance (SPR), which increases the absorption of visible light and encourages the production of reactive oxygen species that break down dyes. Additionally, Ag increases the number of active sites and promotes interfacial electron transport, which raises the total photocatalytic activity [14-18].

$\text{Co}_3\text{O}_4$  nanostructures have been created using a variety of physical and chemical techniques, including sol-gel, hydrothermal, solvothermal, combustion, polyol, thermal decomposition, and polymer-assisted synthesis. Despite the fact that these techniques yield materials with regulated morphology and good crystallinity, they frequently call for expensive precursors, high temperatures, lengthy reaction times, or complex equipment. As an alternative, the co-precipitation approach is a straightforward, inexpensive, scalable, and energy-efficient procedure that may generate uniform nanoparticles with a regulated composition under comparatively mild processing conditions. This approach is ideal for large-scale production and practical applications because it doesn't require surfactants, high pressure, or complicated experimental equipment [19-22].

EBT is an anionic azo dye that is frequently used in analytical chemistry as a complexometric indicator and in textile dyeing. EBT is difficult to break down using traditional treatment techniques and lingers in wastewater for a long time because of its high-water solubility and stable azo (-N=N-) bond. As a result, it is commonly employed as a model pollutant to assess the photocatalytic effectiveness of recently created

\*Corresponding Author: [chemistry.rss@gmail.com](mailto:chemistry.rss@gmail.com) (Rohit Shankar Shinde)



catalysts. Highly reactive species including hydroxyl radicals ( $\bullet\text{OH}$ ) and superoxide radicals ( $\text{O}_2^{\bullet-}$ ), which target the chromophoric groups of the dye molecule and cause its mineralization, are produced during the photocatalytic breakdown of EBT [23-25].

Recent research has shown that a number of operational parameters, including the reaction medium's pH, catalyst dose, initial dye concentration, and irradiation duration, have a significant impact on the photocatalytic efficiency of metal oxide nanoparticles. These elements affect the catalyst's surface charge, light penetration, adsorption-desorption equilibrium, and reactive species production. Therefore, in order to maximize the degradation efficiency and comprehend the photocatalytic mechanism, a methodical examination of these factors is necessary [26,27].

In this study, simple co-precipitation technique has been provided for the economical synthesis of silver-modified cobalt oxide NPs. XRD, FE-SEM, FTIR, EDS, and UV-DRS were used to characterize the structural, morphological, compositional, and optical characteristics of the synthesized NPs. The produced 5% Ag/Co<sub>3</sub>O<sub>4</sub> NPs' photocatalytic activity was assessed for the destruction of EBT dye when exposed to visible light. The degradation kinetics were examined, and the influences of significant reaction parameters like pH, catalyst dosage, and beginning dye concentration were methodically examined. This study is novel since it developed a simple, surfactant-free, and financially feasible synthesis method for Ag-modified Co<sub>3</sub>O<sub>4</sub> NPs with improved photocatalytic performance. This work offers important insights into how adding silver might enhance charge separation and photocatalytic efficiency, which makes the material a viable option for wastewater treatment applications.

## 2. Experimental Methods

### 2.1 Materials

Chemicals such as sodium bicarbonate, cobalt carbonate hexahydrate, silver nitrate, PEG-400, and deionized water were bought from Sigma Laboratory in Nashik and utilized without additional purification.

### 2.2 Synthesis of Nanomaterials

#### 2.2.1 Synthesis of Co<sub>3</sub>O<sub>4</sub> NPs

Cobalt carbonate hexahydrate was used in the precipitation process to create Co<sub>3</sub>O<sub>4</sub> NPs. To create a 0.2 M concentration, the precursor was dissolved in 100 milliliters of deionized water. The 0.2 M NaHCO<sub>3</sub> solution was gradually added while being vigorously stirred until the pH reached 11. At 80 °C, the alkaline solution was agitated using a magnetic stirrer until a grey precipitate formed. Until a neutral condition was achieved, the resulting grey precipitate was filtered and repeatedly cleaned using deionized water and 100% ethanol. The cleaned precipitate was then dried in an oven set to 80 °C for the entire night. Lastly, to produce the Co<sub>3</sub>O<sub>4</sub> NPs, the crude precipitate was calcined for three hours at 450 °C.

#### 2.2.2 Synthesis of 5% Ag-doped Co<sub>3</sub>O<sub>4</sub> NPs

A beaker containing pre-synthesized Co<sub>3</sub>O<sub>4</sub> nanoparticles (95% Co<sub>3</sub>O<sub>4</sub> NPs dispersed in 100 mL of deionized water) was mixed with AgNO<sub>3</sub> corresponding to 5 mol% in order to obtain 5% Ag-doped Co<sub>3</sub>O<sub>4</sub> nanoparticles. Subsequently, 4 mL of PEG-400 was added dropwise as a stabilizing agent. The resulting mixture was stirred at 80 °C for 6 h. The obtained Ag-doped Co<sub>3</sub>O<sub>4</sub> nanoparticles were then filtered, washed several times with deionized water, and dried overnight at 80 °C. Finally, the dried product was calcined at 450 °C for 3 h to obtain crystalline Ag-doped Co<sub>3</sub>O<sub>4</sub> nanoparticles.

## 3. Results and Discussion

### 3.1 Characterization Studies

#### 3.1.1 X-Ray Diffraction Study (XRD)

XRD is an analytical technique mainly used for phase determination of a crystalline material and give knowledge about unit cell dimension. The analysed material is finely ground, homogenized and average bulk composition is determined. X-ray diffractometers contain of three basic elements like an X-ray tube, a sample holder and X-ray detector. The average crystallite size is calculated using a Debye Scherrer's equation [28],  $D = k\lambda/\beta \cos\theta$ ,  $D$  is the mean size of the ordered (crystalline) domains, which may be smaller or equal to the grain size, which may be smaller or equal to the particle size;  $K$  is a dimensionless shape factor, with a value close to unity. The shape factor has a typical value of about 0.9, but varies with the actual shape of the crystallite;  $\lambda$  is the X-ray wavelength;  $\beta$  is the full width at half maximum intensity (FWHM), after subtracting the instrumental line broadening, in radians; and  $\theta$  is the Bragg angle.

<https://doi.org/10.30799/jnst.S301.26110401>

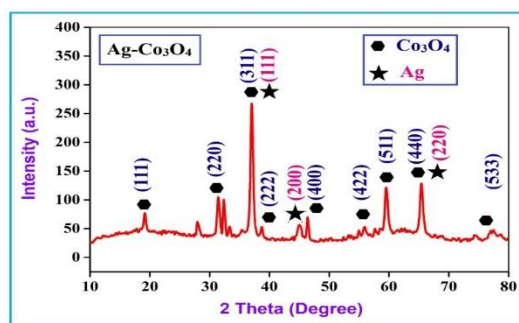


Fig. 1 XRD spectrum of 5% Ag/Co<sub>3</sub>O<sub>4</sub> NPs

By using the above Debye Scherrer equation [29] and XRD graph (Fig. 1), it has been calculated average crystallite size is 18.01 nm. In the case of Co<sub>3</sub>O<sub>4</sub> NPs, the diffraction peaks observed in the Fig. 1 corresponds to the planes (111), (220), (311), (222), (400), (422), (511), (440), and (533). These planes are located at angles  $2\theta = 19.177, 31.424, 37.029, 38.696, 46.322, 56.238, 59.526, 65.451, \text{ and } 77.478$ . The observed peaks correspond to the pure Co<sub>3</sub>O<sub>4</sub> phase with a zinc blende phase and match well with the standard JCPDS file No. 09-0418 [30]. In the case of Ag NPs, the diffraction peaks observed in the Fig. 1 corresponds to the planes (111), (200), and (220). These planes are located at angles  $2\theta = 38.070, 45.057, \text{ and } 65.890$ . The observed peaks correspond to the pure Co<sub>3</sub>O<sub>4</sub> phase with a zinc blende phase and match well with the standard JCPDS file No. 04-0783 [31].

#### 3.1.2 Field Emission - Scanning Electron Microscopy (FE-SEM)

Scanning electron microscopy is widely used to study the morphological features and surface characteristics of catalyst. The 5% Ag/Co<sub>3</sub>O<sub>4</sub> nanocomposites were analysed by SEM. Fig. 2 shows sphere like morphology of 5% Ag/Co<sub>3</sub>O<sub>4</sub>. The agglomerates were purely due to the magnetic induction between the particles.

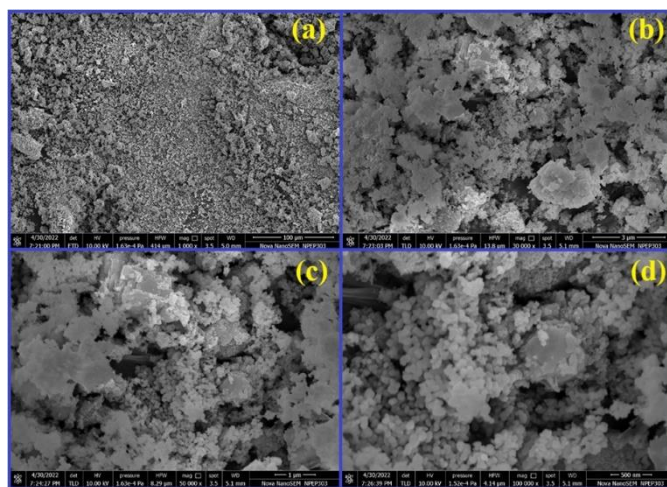


Fig. 2 FE-SEM analysis of 5% Ag/Co<sub>3</sub>O<sub>4</sub> NPs

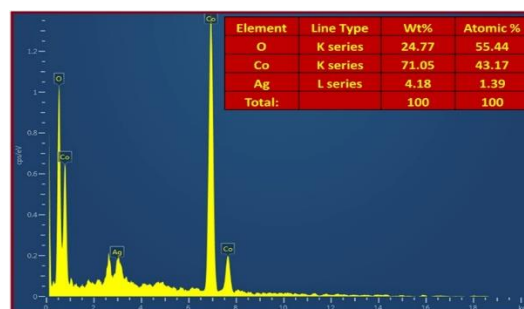


Fig. 3 EDS spectrum of 5% Ag/Co<sub>3</sub>O<sub>4</sub> NPs

#### 3.1.3 Energy Dispersive Spectroscopy (EDS)

The elemental composition of the synthesized 5% Ag/Co<sub>3</sub>O<sub>4</sub> nanoparticles was examined by energy-dispersive X-ray spectroscopy (EDS), and the corresponding spectrum is presented in Fig. 3. The spectrum clearly confirms the presence of cobalt, oxygen, and silver without any detectable impurity peaks, demonstrating the high purity of the prepared sample. Quantitative analysis reveals that Co and O are the

major constituents with weight percentages of 71.05% and 24.77%, respectively, while Ag is present in a smaller amount (4.18 wt%), which is consistent with the intended dopant concentration. The corresponding atomic percentages (Co: 43.17%, O: 55.44%, Ag: 1.39%) further support the formation of the cobalt oxide framework with successful incorporation of silver.

In the EDS spectrum, the characteristic peaks of cobalt are observed at approximately 6.9 and 7.6 keV, which are attributed to the Co K $\alpha$  and Co K $\beta$  transitions associated with Co<sup>2+</sup> and Co<sup>3+</sup> species in the spinel Co<sub>3</sub>O<sub>4</sub> lattice. The strong oxygen signal appearing around 0.5 keV corresponds to the O K $\alpha$  emission, confirming the oxide nature of the material. In addition, the appearance of a distinct peak at ~3.0 keV is assigned to the Ag L $\alpha$  transition, providing clear evidence for the presence of silver in the modified sample. The absence of additional peaks related to other elements indicates that the doping process did not introduce any secondary phases or contaminants.

The relative intensity of the Ag peak compared with those of Co and O suggests that silver is present in a low concentration and is well dispersed on the Co<sub>3</sub>O<sub>4</sub> matrix rather than forming a separate bulk phase. Such a homogeneous distribution of Ag is beneficial for catalytic and surface-dependent applications, as it can enhance the number of active sites and improve electron transfer characteristics. Overall, the EDS results confirm the successful formation of phase-pure 5% Ag/Co<sub>3</sub>O<sub>4</sub> nanoparticles with effective incorporation of Ag into the cobalt oxide system, in good agreement with the nominal composition.

### 3.1.4 Fourier Transform Infrared Spectroscopy (FTIR)

The FT-IR spectrum of the synthesized 5% Ag/Co<sub>3</sub>O<sub>4</sub> nanoparticles (Fig. 4) exhibits the characteristic vibrational bands of the spinel Co<sub>3</sub>O<sub>4</sub> structure, confirming the formation of the metal–oxygen framework. Two prominent absorption bands are observed at 663.39 and 568.89 cm<sup>-1</sup>, which are attributed to the intrinsic stretching vibrations of cobalt–oxygen bonds in the spinel lattice. The higher wavenumber band at 663.39 cm<sup>-1</sup> corresponds to the Co<sup>2+</sup>–O stretching vibration at the octahedral site, while the band at 568.89 cm<sup>-1</sup> is associated with the bridging O–Co–O vibration, typically assigned to the Co<sup>3+</sup>–O stretching mode at the tetrahedral site. These bands are the fingerprint features of Co<sub>3</sub>O<sub>4</sub> and indicate the preservation of the cubic spinel structure after silver incorporation.

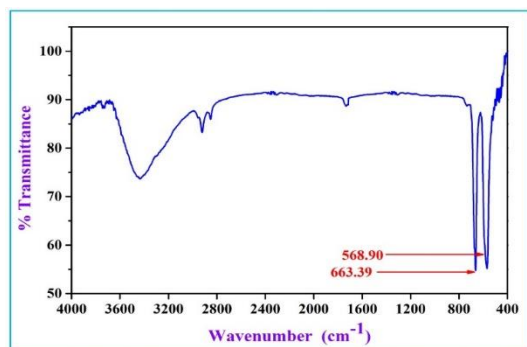


Fig. 4 FTIR spectrum of 5% Ag/Co<sub>3</sub>O<sub>4</sub> NPs

### 3.1.5 UV-DRS Study

The optical properties of the synthesized 5% Ag/Co<sub>3</sub>O<sub>4</sub> nanoparticles were investigated using UV–visible diffuse reflectance spectroscopy in the wavelength range of 200–800 nm, and the corresponding spectrum is shown in Fig. 5(a). The material exhibits strong absorption in the UV region with a noticeable extension toward the visible region, indicating its ability to harvest a broad range of the solar spectrum. The observed absorption edge is mainly associated with the charge transfer transitions between O<sup>2-</sup> and Co<sup>3+</sup> ions in the spinel Co<sub>3</sub>O<sub>4</sub> lattice. A distinct photoluminescence emission peak at 290 nm is observed, which originates from the free excitonic recombination process. The presence of emission in the visible region further suggests the existence of defect states and surface energy levels introduced by Ag incorporation, which can act as trapping centers for photogenerated charge carriers and thereby influence the recombination dynamics. Such an extended absorption behavior and defect-mediated electronic transitions are beneficial for photocatalytic and photo-assisted applications. The optical band gap energy of the 5% Ag/Co<sub>3</sub>O<sub>4</sub> nanoparticles was estimated using the Tauc relation, and the corresponding plot of (ahv)<sup>2</sup> versus photon energy (hv) is presented in Fig. 4(b). By extrapolating the linear portion of the curve to the energy axis, the band gap was determined to be 3.01 eV, confirming the semiconducting nature of the material. The slight modification in the band

structure compared to pristine Co<sub>3</sub>O<sub>4</sub> can be attributed to the electronic interaction between Ag and the Co<sub>3</sub>O<sub>4</sub> matrix, which leads to the formation of intermediate energy levels and improved charge transfer characteristics. This narrowing/adjustment of the band gap facilitates enhanced visible-light absorption and suppresses the rapid recombination of photogenerated electron–hole pairs, thereby improving the overall photocatalytic efficiency of the Ag-modified Co<sub>3</sub>O<sub>4</sub> system.

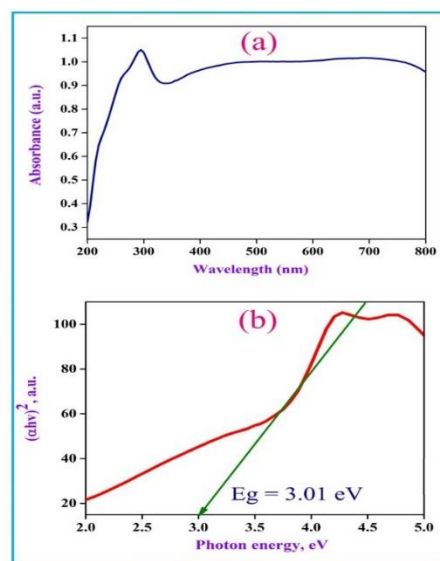


Fig. 5 (a) The UV-DRS and optical band gap spectrum and (b) Tauc plot of 5% Ag/Co<sub>3</sub>O<sub>4</sub> NPs

## 3.2 Photo-Degradation Study of EBT Dye using 5% Ag/Co<sub>3</sub>O<sub>4</sub> NPs

### 3.2.1 Effect of pH

The effect of pH on the photocatalytic degradation of EBT dye using 5% Ag/Co<sub>3</sub>O<sub>4</sub> nanoparticles was systematically investigated in the pH range of 2–10 at an initial dye concentration of 10 mg/L with a catalyst dosage of 1 g/L for an irradiation time of 60 min, and the results are presented in Fig. 6. The degradation efficiency was found to be strongly dependent on the solution pH, with the maximum removal achieved at pH 6. At highly acidic and alkaline conditions, a noticeable decrease in photocatalytic activity was observed. This variation in degradation efficiency can be attributed to changes in the surface charge of the catalyst, the degree of ionization of the dye molecules, and the generation of reactive oxygen species under different pH conditions.

At lower pH values, the catalyst surface becomes positively charged due to protonation, which leads to reduced interaction with the dye molecules and limits the formation of hydroxyl radicals, thereby lowering the degradation efficiency. In contrast, in highly alkaline media, the excess OH<sup>-</sup> ions may act as scavengers for photogenerated holes and hydroxyl radicals, resulting in a decreased photocatalytic performance. The enhanced degradation at near-neutral pH (pH 6) is attributed to the optimum electrostatic interaction between the catalyst surface and the dye molecules, along with efficient generation of reactive species such as •OH radicals. Therefore, pH 6 was considered the optimum condition for the photocatalytic degradation of EBT dye using 5% Ag/Co<sub>3</sub>O<sub>4</sub> NPs.

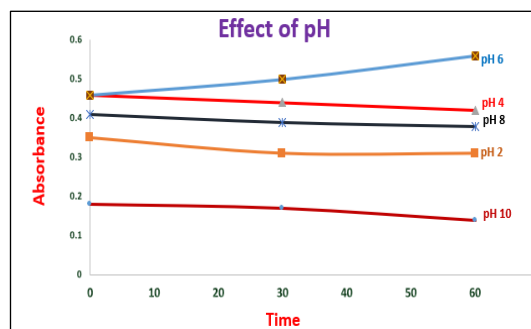


Fig. 6 Effect of pH on photocatalytic degradation of EBT dye using 5% Ag/Co<sub>3</sub>O<sub>4</sub> NPs

### 3.2.2 Effect of Initial Dye Concentration

The effect of the initial Eriochrome Black T (EBT) dye concentration on the photocatalytic degradation efficiency of 5% Ag/Co<sub>3</sub>O<sub>4</sub> nanoparticles was investigated by varying the dye concentration in the range of 5–20

mg/L under the optimized pH condition (pH = 6), and the results are presented in Fig. 7. It was observed that the degradation efficiency decreased with an increase in the initial dye concentration. The maximum degradation was achieved at the lowest dye concentration, while a gradual decline in photocatalytic performance was recorded at higher concentrations. This behavior indicates that the photocatalytic process is strongly influenced by the availability of active sites on the catalyst surface as well as the penetration of light into the reaction medium.

At lower dye concentrations, the number of dye molecules is relatively small compared to the available active sites on the catalyst surface, allowing efficient adsorption and subsequent generation of reactive oxygen species for effective degradation. However, at higher concentrations, a larger number of dye molecules compete for the limited active sites, leading to surface saturation and reduced formation of hydroxyl and superoxide radicals. In addition, the increased dye concentration causes a shielding effect, which limits the transmission of incident light to the catalyst surface and thereby decreases the generation of photogenerated electron-hole pairs. Consequently, the photocatalytic degradation efficiency decreases with increasing initial dye concentration, confirming that lower dye concentrations are more favorable for efficient photocatalytic activity of 5% Ag/Co<sub>3</sub>O<sub>4</sub> nanoparticles.

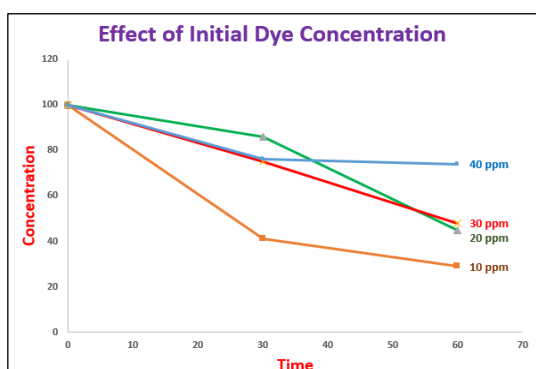


**Fig. 7** Effect of initial dye concentration on photocatalytic degradation of EBT dye using 5% Ag/Co<sub>3</sub>O<sub>4</sub> NPs

### 3.2.3 Effect of Catalyst Dose

The effect of catalyst dosage on the photocatalytic degradation of Eriochrome Black T (EBT) dye was examined by varying the amount of 5% Ag/Co<sub>3</sub>O<sub>4</sub> nanoparticles from 0.2 to 1.0 g/L while keeping other operational parameters constant, such as pH, initial dye concentration, and irradiation time. The results, presented in Fig. 8, clearly show that the degradation efficiency increases with increasing catalyst dose and reaches a maximum at 1.0 g/L. The enhancement in photocatalytic activity with higher catalyst loading is mainly attributed to the increase in the number of available active sites and the larger effective surface area, which promotes greater adsorption of dye molecules and more efficient generation of reactive oxygen species under light irradiation.

At lower catalyst dosages, the number of active sites is limited, resulting in reduced interaction between the catalyst and dye molecules and consequently lower degradation efficiency. As the catalyst amount increases, more photons are absorbed and a higher number of electrons-hole pairs are generated, leading to improved formation of hydroxyl and superoxide radicals responsible for dye degradation. However, beyond an optimum dosage, further increase in catalyst concentration may cause particle agglomeration and light scattering, which can reduce the penetration of light into the reaction medium and lower the photocatalytic efficiency. Therefore, 1.0 g/L was considered the optimum catalyst dose for the effective degradation of EBT dye using 5% Ag/Co<sub>3</sub>O<sub>4</sub> nanoparticles.

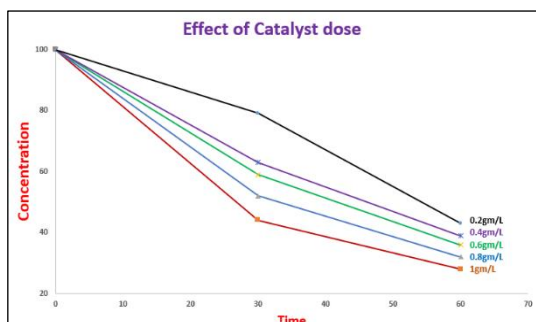


**Fig. 8** Effect of catalyst dose on photocatalytic degradation of EBT dye using 5% Ag/Co<sub>3</sub>O<sub>4</sub> NPs

<https://doi.org/10.30799/jnst.S301.26110401>

## 4. Conclusion

Nanoparticles of 5% Ag/Co<sub>3</sub>O<sub>4</sub> were successfully synthesized by a cost-effective co-precipitation method. The structural, morphological, and optical properties of the prepared nanoparticles were characterized using XRD, FE-SEM, FT-IR, EDS, and UV-DRS techniques. The XRD results confirmed the crystalline nature of the material with an average crystallite size of 18.01 nm. FE-SEM analysis revealed that the synthesized nanoparticles possess a nearly spherical morphology. The successful incorporation of Ag into the Co<sub>3</sub>O<sub>4</sub> lattice was verified by EDS analysis. FT-IR spectra exhibited characteristic absorption bands at 663.39 and 568.89 cm<sup>-1</sup>, corresponding to Co–O and O–Co–O stretching vibrations of the spinel Co<sub>3</sub>O<sub>4</sub> structure. UV-DRS analysis indicated an optical band gap of 3.01 eV for the 5% Ag/Co<sub>3</sub>O<sub>4</sub> nanoparticles.

The photocatalytic activity of the synthesized catalyst was evaluated through the degradation of EBT dye under optimized conditions. Maximum degradation efficiency was achieved at pH 6 using a catalyst dose of 1 g/L, resulting in nearly 75% dye removal. The effects of operational parameters such as initial dye concentration, catalyst dosage, and solution pH were systematically investigated. The enhanced photocatalytic performance is attributed to the synergistic effect of Ag incorporation, which improves light absorption and suppresses the recombination of photogenerated charge carriers. These results demonstrate that 5% Ag/Co<sub>3</sub>O<sub>4</sub> nanoparticles are an efficient and promising photocatalyst for dye degradation in wastewater treatment.

## Acknowledgement

The authors are thankful to the management of Mahatma Gandhi Vidyamandir's ASC College, Manmad for providing the necessary research facilities. The authors also acknowledge SAIF, Cochin University, Kerala for XRD, EDS, and SEM analyses. The authors are grateful to Jaysingpur College, Jaysingpur for FTIR and UV-DRS measurements.

## References

- [1] V. Saxena, Water quality, air pollution, and climate change: investigating the environmental impacts of industrialization and urbanization, *Water Air Soil Pollut.* 236 (2025) 73.
- [2] M. Mehta, M. Sharma, K. Pathania, P.K. Jena, I. Bhushan, Degradation of synthetic dyes using nanoparticles: a mini-review, *Environ. Sci. Pollut. Res.* 28 (2021) 49434–49446.
- [3] S. Dave, J. Das, B. Varshney, V.P. Sharma, Dyes and pigments: interventions and how safe and sustainable are colors of life!!!, in: *Trends and contemporary technologies for photocatalytic degradation of dyes*, Springer Int. Publ., Cham, 2022, pp.1–20.
- [4] J. Kaur, S. Tewari, A. Kaur, R. Malik, Dye and dye-containing hazardous waste in water resource, in: *Emerging contaminants in water and wastewater: Sources and Substances*, Springer Nature Switzerland, Cham, 2025, pp.179–199.
- [5] J. Awewomom, F. Dzeble, Y.D. Takyi, W.B. Ashie, E.N.Y.O. Ettey, et al., Addressing global environmental pollution using environmental control techniques: a focus on environmental policy and preventive environmental management, *Discover Environ.* 2 (2024) 8.
- [6] K. Mishra, N. Devi, S.S. Siwal, V.K. Gupta, V.K. Thakur, Hybrid semiconductor photocatalyst nanomaterials for energy and environmental applications: fundamentals, designing, and prospects, *Adv. Sustain. Syst.* 7 (2023) 2300095.
- [7] R. Tiwari, A.R. Zala, P. Kumari, Remediation of wastewater through photo-induced catalytic and electrochemical hydrogen production, in: *Synergy of bio-chemical processes for photocatalytic and photoelectrochemical wastewater treatment*, 2024, pp. 139–160.
- [8] B. Karthikeyan, G. Gnanakumar, A.T. Alphonsa, Nano metal oxides: Engineering and biomedical applications, Springer Nature Singapore, Singapore, 2023.
- [9] P.K. Panigrahi, B. Chandu, N. Puvvada, Recent advances in nanostructured materials for application as gas sensors, *ACS Omega* 9 (2024) 3092–3122.
- [10] S. Kumar, A. Kaur, J. Gaur, P. Singh, H. Kaur, et al., State-of-the-art in Co<sub>3</sub>O<sub>4</sub> nanoparticle synthesis and applications: toward a sustainable future, *Chemistry Select* 10 (2025) e202405147.
- [11] M. Alzaid, A.M. Abu-Dief, N.M.A. Hadia, M. Ezzeldien, W.S. Mohamed, Synthesis and characterization study of spinel Co<sub>3</sub>O<sub>4</sub> nanoparticles synthesized via the facile co-precipitation route for optoelectronic application, *Opt. Quantum Electron.* 56 (2024) 1156.
- [12] Ravina, G. Srivastava, S. Dalela, S. Kumar, M. Nasit, et al., Study of structural, optical, surface and electrochemical properties of Co<sub>3</sub>O<sub>4</sub> nanoparticles for energy storage applications, *Interactions* 245 (2024) 85.
- [13] F. Zhao, H. Ma, Application of Co<sub>3</sub>O<sub>4</sub> in photoelectrocatalytic treatment of wastewater polluted with organic compounds: a review, *Crystals* 13 (2023) 634.
- [14] Y. Ali, M. Hilal, O. Khan, Z.U. Rehman, S.T. Din, S. Lee, Challenges, prospects, and surface chemistry of CuCo<sub>2</sub>O<sub>4</sub> in energy storage, electro-photocatalysis, solar cells, and sensor applications, *J. Mater. Sci.: Mater. Electron.* 36 (2025) 1189.
- [15] M. Humayun, C. Wang, W. Luo, Recent progress in the synthesis and applications of composite photocatalysts: a critical review, *Small Methods* 6 (2022) 2101395.

- [16] F. Nasim, H. Malik, G. Xu, H. Dong, M.A. Nadeem, Exploring the heterointerface of silver nanoparticles and cobalt oxide nanorings toward the oxygen reduction reaction, *J. Mater. Chem. A* 13 (2025) 23981–23997.
- [17] R. Kumar, S.Y. Janbandhu, G.K. Sukhadeve, R.S. Gedam, Visible light assisted surface plasmon resonance triggered Ag/ZnO nanocomposites: synthesis and performance towards degradation of indigo carmine dye, *Environ. Sci. Pollut. Res.* 30 (2023) 98619–98631.
- [18] B. Xin, L. Jing, Z. Ren, B. Wang, H. Fu, Effects of simultaneously doped and deposited Ag on the photocatalytic activity and surface states of TiO<sub>2</sub>, *J. Phys. Chem. B* 109 (2005) 2805–2809.
- [19] X. Wang, A. Hu, C. Meng, C. Wu, S. Yang, X. Hong, Recent advance in Co<sub>3</sub>O<sub>4</sub> and Co<sub>3</sub>O<sub>4</sub>-containing electrode materials for high-performance supercapacitors, *Molecules* 25 (2020) 269.
- [20] H. Lan, J. Wang, L. Cheng, D. Yu, H. Wang, L. Guo, The synthesis and application of crystalline–amorphous hybrid materials, *Chem. Soc. Rev.* 53 (2024) 684–713.
- [21] S. Viswanathan, T.S. Adithya, M. Chandana, Synthesis, characterization, and properties of nanomaterials, in: *Advanced nanomaterials and composites: Vol.1*, Springer Nature Singapore, Singapore, 2026, pp.37–63.
- [22] T. Tiso, P. Demling, T. Karmainski, A. Oraby, J. Eiken, et al., Foam control in biotechnological processes - challenges and opportunities, *Discover Chem. Eng.* 4 (2024) 2.
- [23] H. Naz, H. Vaseem, Evaluation of hepatotoxic potential of an azo dye, eriochrome black-T on freshwater catfish, *Clarias batrachus*, *Bull. Environ. Contam. Toxicol.* 114 (2025) 9.
- [24] F. Salimi, V. Valiei, C. Karami, Removal of EBT dye from aqueous solution by modified MoNiO<sub>4</sub> adsorbent, *Desalin. Water Treat.* 190 (2020) 340–352.
- [25] A. Iqbal, A. Yusaf, M. Usman, T. Hussain Bokhari, A. Mansha, Insight into the degradation of different classes of dyes by advanced oxidation processes: a detailed review, *Int. J. Environ. Anal. Chem.* 104 (2024) 5503–5537.
- [26] T. Sarkar, A. Bhattacharjee, Green synthesized ZnO nanocatalysts for rapid and effective visible-light degradation of industrial dyes, *RSC Adv.* 16 (2026) 2671–2684.
- [27] K. Nagaraja, B. Mallika, M. Arunpandian, N. Macherla, T.H. Oh, Green-engineered rare-earth-doped ZnO–Y<sub>2</sub>O<sub>3</sub> nanocomposites for efficient textile dye degradation: operational parameter, environmental toxicity evaluation, and agricultural safety assessment, *Colloids Surf. A* 189 (2026) 139664.
- [28] R.S. Shinde, S.D. Khairnar, M.R. Patil, V.A. Adole, P.B. Koli, et al., Synthesis and characterization of ZnO/CuO nanocomposites as an effective photocatalyst and gas sensor for environmental remediation, *J. Inorg. Organomet. Polym. Mater.* 32 (2022) 1045–1066.
- [29] R.S. Shinde, V.A. Adole, S.D. Khairnar, P.B. Koli, T.B. Pawar, Study of Fe<sub>3</sub>O<sub>4</sub> and Cu<sup>2+</sup>-doped modified Fe<sub>3</sub>O<sub>4</sub> nanocatalyst for photocatalytic degradation of methylene blue and eriochrome black-T dyes: synthesis, characterization, and antimicrobial assessment, *Inorg. Chem. Commun.* 170 (2024) 113206.
- [30] S. Rathod, K.K. Joshi, P.M. Pataniya, C.K. Sumesh, S. Kapatel, Nb doping strategy for active site modification in Co<sub>3</sub>O<sub>4</sub> to enable concurrent hydrogen production and glycerol valorization for efficient formate production, *J. Mater. Chem. A* 14 (2026) 4268–4281.
- [31] H.A.B. Saeed, N. Sajjad, Z. Zulfiqar, Z. Fatima, M.A. Hussain, et al., Eco-friendly fabrication of silver nanoparticles from *Echinops* species: a comparative study of antibacterial and photocatalytic performance, *RSC Adv.* 16 (2026) 7603–7617.